International Forum on Aeroelasticity and Structural Dynamics
IFASD 2024
17-21 June 2024, The Hague, The Netherlands

GUST LOAD ALLEVIATION EFFICIENCY IN AN OPTIMIZED COMPOSITE WING THROUGH THE INTEGRATION OF WINGTIP DEVICES: INCORPORATING FOLDING AND TWIST STRATEGIES

Touraj Farsadi[1,2], Majid Ahmadi[1] and Hamed Haddad Khodaparast[2]

[1] Swansea University, Aerospace Engineering Department, UK
[2] Adana Alparslan Turkes Science and Technology University, Aerospace Engineering Department, Türkiye

Keywords: Gust load alleviation, Aeroelasticity, Wingtip device, Composite wing

Abstract: This paper presents a numerical methodology for designing and studying high aspect ratio composite baseline wings equipped with passive control systems, namely Folding WingTip (FWT) and Twist WingTip (TWT) devices, with the primary objective of enhancing gust load alleviation. The methodology integrates Finite Element (FE) software and a Reduced Order Model (ROM) framework for dynamic aeroelastic analyses, all within the Nonlinear Aeroelastic Simulation Software (NAS^2) package, facilitating streamlined aeroelastic design of composite wings equipped with wingtip devices. NAS^2 serves as a reliable and efficient platform for coupling diverse simulation codes, thereby enabling precise simulation of the interaction between aerodynamics and structures. To examine the impact of wingtip devices, we will use a previously established baseline wing design [7]. The design aimed to optimize high aspect ratio composite wings by minimizing weight while considering structural, material, aeroelastic, and manufacturing limitations. The baseline wing is equipped with Folding Wingtip (FWT) and Twist Wingtip (TWT) devices to study their impact on Gust Load Alleviation (GLA). The present study evaluates the effectiveness of these wingtip devices in reducing gust load, with a particular focus on the root bending moment. It allows for a comprehensive comparison of gust responses between the baseline wing and the wing equipped with these passive wingtip devices.

1 INTRODUCTION

Gust loading poses a significant challenge for high aspect ratio wings, which are particularly vulnerable due to their elongated and slender structure. These wings' flexibility can cause deformations that adversely affect both their aerodynamic efficiency and structural integrity [1-6]. However, the adoption of wingtip devices such as Folding WingTip (FWT) and Twist WingTip (TWT) offers an effective solution for Gust Load Alleviation (GLA). These devices adjust the aerodynamic properties of the wing, decreasing its sensitivity to gusts and minimizing the risk of intense localized aerodynamic forces. By altering the distribution of lift along the wing's span, wingtip devices effectively reduce the impact of gust-induced loads, enhancing passenger comfort and reducing structural stress on the wing. This forward-thinking strategy not only improves the design and functionality of high aspect ratio wings but also supports the creation of lighter, more fuel-efficient, and environmentally sustainable aircraft. The Root Bending Moment (RBM) is

crucial for maintaining the structural integrity of an aircraft wing during gust loading and is heavily dependent on the wing's weight. A lighter wing often exhibits a lower RBM due to its reduced mass and increased sensitivity to aerodynamic forces. In contrast, a heavier wing, while resistant to deformation, experiences larger bending moments. Consequently, efficient GLA can play a significant role in facilitating the development of lighter, more fuel-efficient, and environmentally sustainable aircraft.

The numerical investigations conducted by Castrichini et al. [8] demonstrated that the FWT design effectively reduces the Wing Root Bending Moment (WRBM) and offers a mechanism for alleviating gust loads. Gu et al. [9] developed Semi-Aeroelastic Hinge (SAH) devices for high aspect ratio wings, which allow aircraft to fit into airport gates and reduce aerodynamic loads using floating wingtips. Incorporating SAH devices with a 30% relative floating wingtip span resulted in a 25% reduction in wing weight and over a 5% improvement in aircraft range. Healy et al. [10] studied the nonlinear dynamics of wings with Flared Folding WingTips (FFWTs). Their study investigated the impact of a wingtip trim tab and suggested that a movable control surface on FFWTs can expand the stability boundary. Corcoles et al. [11] examined the influence of wing stiffness and hinge release on GLA in FWT designs, showing that hinge release timing played a significant role in reducing peak loads, albeit affecting system dynamics. They recommended further investigations into flutter velocities, nonlinear aeroelastic models, and combinations with other GLA mechanisms. Cheung et al. [12] explored FWTs for flexible, high aspect ratio wing, where wind tunnel tests demonstrated up to an 56% reduction in peak rolling moment when compared with the stiff-hinge baseline. Balatti et. al. [13] employed a genetic algorithm to optimize wingtip parameters for minimizing gust response while maintaining a safe flutter speed. Wingtip rotation reduced bending and torsional deflection, thereby improving stability. Various configurations, including adjustments in springs and flare angle, enhanced flutter speed and GLA. Balatti et al. [14] validated aeroelastic models of wings with hinged wingtips in a wind tunnel. Tests confirmed their effectiveness in reducing gust loads and led to a more efficient wingtip design. Adjustments in wingtip mass, center of mass position, and hinge stiffness effectively reduced wing RBM. Ajaj et. al. [15] conducted a parametric study on the aeroelasticity of cantilever wings with Flared Hinge Folding WingTips (FHFWTs). They developed a low-fidelity finite element aeroelastic model using Euler–Bernoulli beam elements for the wing structure and Theodorsen's aerodynamic strip theory for load predictions. The study demonstrates that FHFWTs expand the aeroelastic envelope, reducing RBM and shear force.

He et. al. [16] evaluated the effectiveness of a Passive Gust Alleviation Device (PGAD) with a TWT installed on a large flying-wing aircraft. Numerical analysis and wind tunnel testing of a scaled model confirmed the TWT's effectiveness, reducing the gust response by 9%. Guo et. al. [17] assessed a PGAD installed on the wingtip of a small, high-aspect-ratio flying-wing aircraft. The PGAD decreased the gust-induced bending moment at the wing root by 16% and increased Body Freedom Flutter (BFF) speed by 4.2%.

The present work evaluates the effectiveness of folding and twist wingtip devices in reducing gust load on the baseline wing [7], with particular attention to the root bending moment as an interesting quantity. The incorporation of these devices at the end of the baseline wing facilitates a detailed comparison of gust responses between the baseline wing and the wing equipped with the Folding and Twist wingtip devices. The systematic approach presented here, innovative wingtip devices, serves as a valuable tool for designing lightweight wings with improved aeroelastic and structural

performance, thus advancing the field of high aspect ratio wing configurations in aerospace engineering.

2 BASELINE WING CONFIGURATION

The primary aim of this work is to provide an enhanced aeroelastic scenario that improves the performance of aircraft wings when subjected to gust loading and turbulence. This is accomplished by employing an optimal hinge shape, where the Folding WingTip (FWT) and Twist WingTip (TWT) serve as passive devices to reduce gust-induced loads. The FWT provides benefits due to the geometric relationship between the direction of the folding axis and the resulting change in the effective angle of attack as the wingtip folds. By twisting the wingtip, the angle of attack in that specific area is reduced, which changes how lift is distributed across the span of the wing. This is done in order to minimize the drag caused by the wing's induced airflow. This technique aims to optimize the spanload curve by considering its present properties.

The geometrical and layup stacking sequence configuration of the composite high aspect ratio baseline wing model were initially derived from the authors' previous works reported in Ref [7]. The optimization process involves configuring the placement, including fiber orientation and order, across three regions along the span. The ultimate goal is to simultaneously enhance performance in terms of structural integrity and aeroelasticity while minimizing weight. Initially, a preliminary structural design of the wing was carried out, followed by structural composite analysis and aeroelastic analysis. For further investigation, a composite wing with specifications listed in Table 1 and a schematic description shown in Figure 1 is chosen as the baseline wing. In Figure 1, the lengths along the span in the upper skin are denoted as L_1^U, L_2^U and L_3^U, while in the lower skin, they are represented as L_1^L, L_2^L and L_3^L.

Table 1: Specifications of the wing under investigation

Half span	1250 mm
Leading edge sweep angle	0 degrees
Front spar location, % chord	25
Number of Ribs	10
Wing aspect ratio	14
Taper ratio	1
Airfoil	NACA 0010

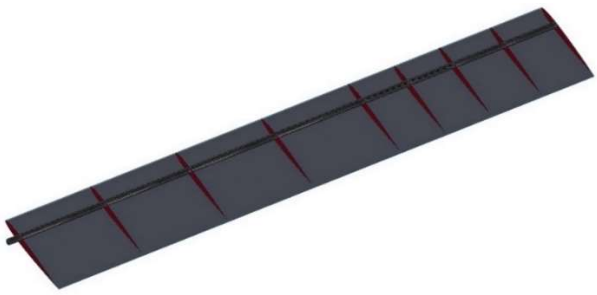

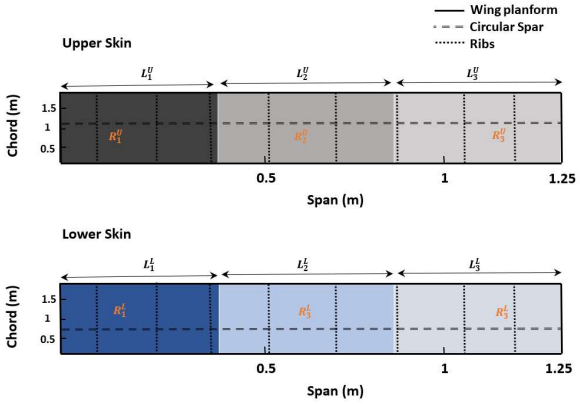

Figure 1. Graphical representation and photograph of the manufactured wing in the baseline wing configuration used as a case study. The design regions are indicated by different colors in the upper and lower skins [7].

3 GUST LOAD ALLEVIATION DEVICES

The long and slender design of high aspect ratio wings renders them very vulnerable to the impact of gusts, which presents considerable difficulties. When the wing experiences gusts, it undergoes increased aerodynamic loads, resulting in higher stresses and the possibility of structural deformation. High aspect ratio wings possess a flexible quality that allows them to undergo deformation when exposed to gust loads, which can negatively impact both their aerodynamic efficiency and structural strength. In order to alleviate these symptoms, a variety of methods are utilized. Aircraft design approaches, such as FWT and TWT, have a substantial impact on the Gust Load Alleviation (GLA) in wings with a high aspect ratio [18].

Wingtip devices modify the way lift is distributed over the wing, making it less affected by gusts and minimizing the chance of strong aerodynamic forces near the wingtip. They also enhance the ability of the wing to reduce abrupt changes in airflow. Significantly, although the aeroelastic gradient is decreased, the aerodynamic gradient stays unaltered.

3.1 Folding WingTip (FWT)

In a FWT configuration, increasing the fold angle reduces the local Angle of Attack (AoA), while decreasing the fold angle increases the local AoA. Consequently, when a foldable wingtip is allowed to rotate, it naturally converges towards an equilibrium position known as the coast angle. At this coast angle, the balance of aerodynamic and gravitational moments makes the system statically stable. This inherent stability ensures that the folding wingtip maintains a steady position, optimizing overall aerodynamic performance and operational safety.

For a visual representation, please refer to Figure 2, which illustrate the schematic depiction of wings equipped with FWT. k_β represents torsional spring stiffness in FWT.

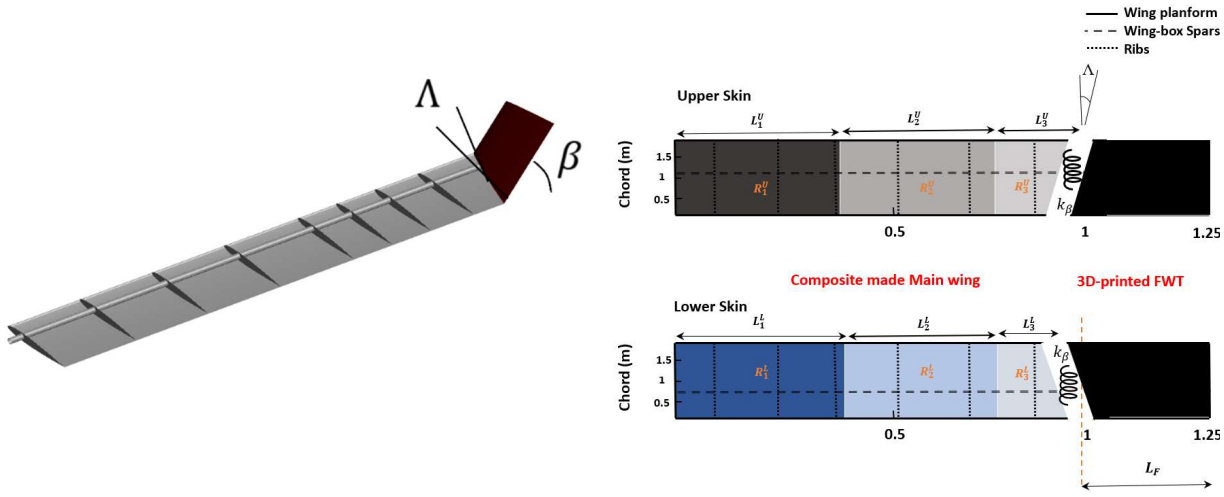

Figure 2. Schematic representation of Folding wing with integrated spring mechanism

3.2 Twist WingTip (TWT)

As the aircraft encounters gusts or turbulent air, the passive TWT deforms, causing it to twist. This deformation, due to the wingtip's inherent flexibility, changes the local angle of attack, redistributing aerodynamic loads along the wing span. The passive TWT's response to varying airflow conditions mitigates the impact of gusts on the aircraft's structural components, particularly at the wing tips. Acting as a self-adjusting system, the passive TWT dynamically alters its shape to optimize aerodynamic performance and enhance stability during turbulence. Please refer to Figures 3, which illustrate the schematic depiction of wing equipped with TWT. The rotational spring stiffness in TWT is denoted by k_θ.

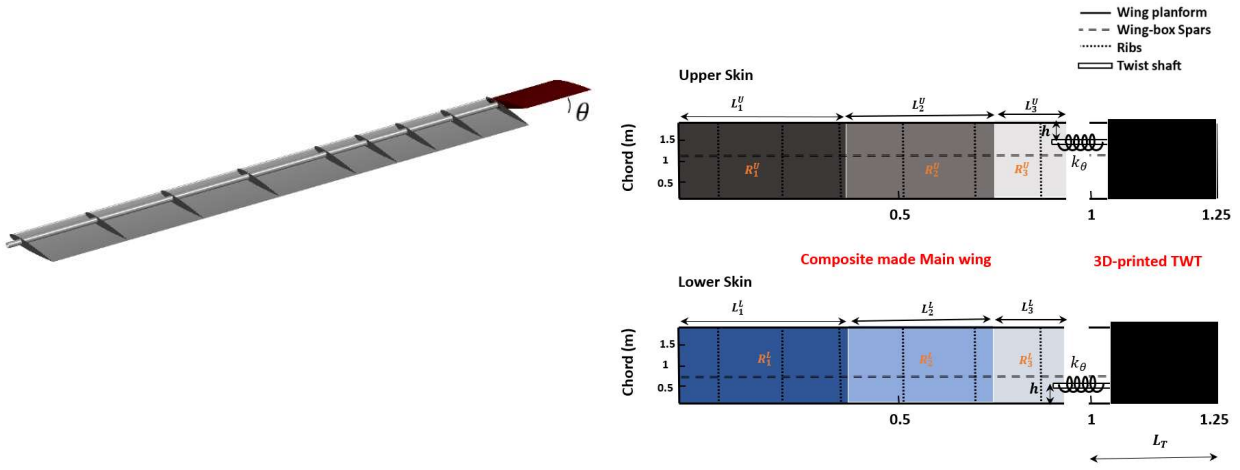

Figure 3. Schematic representation of the Twist wingtip with integrated spring mechanism

4 METHODOLOGY

The NAS^2 software automation process [6,7] is an integrated software package that can be utilized for aeroelastic analysis. It serves as a helpful tool in the design process of the current composite wing model. Using ANSYS Mechanical for structural analysis and a 3D panel aerodynamic method for static analysis, along with ZAERO's VLM code for gust analysis, is a valid and practical approach for comprehensive aeroelastic analysis of the high aspect ratio wing with wingtip devices. The two-way coupling technique for large deflection static aeroelastic analysis followed by modal analysis from the resulting nonlinear static state to perform gust analysis with a reduced-order model (ROM) leverages the strengths of each method. This hybrid approach effectively captures detailed static deformation and dynamic responses to gusts. The ROM's adaptability to various gust profiles and dynamic loading conditions offers flexibility in aeroelastic analysis.

A ROM is constructed using the mode shapes and frequencies (typically 10 modes) derived from the modal analysis performed in ANSYS. Aerodynamic effects are integrated using ZAERO's VLM code to account for gust interactions, and the ROM is validated against known solutions or high-fidelity simulations to ensure the structure's dynamics are accurately captured. Gust inputs, such as the 1-cosine gust profile, is defined, and the structure's dynamic response is simulated using the ROM. This approach enables rapid simulations, facilitating extensive parametric studies and sensitivity analyses.

4.1 Reduced Order gust analysis

First, a detailed finite element model (FEM) of the folding wing is created using ANSYS. This model includes the definition of material properties, boundary conditions, and hinge locations for the folding and twist mechanism. A static analysis is conducted to capture the initial nonlinear large deformations and stresses within the wing structure [7]. Following this, a modal analysis is performed to extract the natural frequencies ω_n and mode shapes ϕ_n. The governing equation for free vibration in this context is $\mathbf{K}\phi_n = \omega_n^2\mathbf{M}\phi_n$ where $\mathbf{K}$ represents the stiffness matrix, $\mathbf{M}$ the mass matrix, and ϕ_n the mode shape corresponding to the natural frequency ω_n. Next, the unsteady aerodynamic forces acting on the wing are calculated using ZAERO's Vortex Lattice Method (VLM). The aerodynamic influence coefficients (AIC) matrix $\mathbf{Q}(k)$ for reduced frequency k is employed to relate the aerodynamic pressures to the wing deflections. To account for the gust loads, the 1-cosine gust vertical speed profile (V_g) is defined as;

$$\frac{V_g}{V} = \begin{cases} \frac{WG}{2}[1-\cos(2\pi F t)], & t < T \\ 0, & t \geq T \end{cases} \tag{1}$$

and, $F = \frac{1}{T}$, $T = \frac{2H}{V}$, $WG = \frac{V_{ds}}{V}$.

where, V_{ds} is the peak gust velocity, V the forward inflow speed, $2H$ the gust length and F corresponds to the gust frequency. WG is the relative intensity of a gust with respect to the inflow speed of the aircraft. A higher WG indicates a stronger gust and a more significant disturbance to

the airflow, while a lower WG signifies a weaker gust and a less significant disturbance. Figure 4 illustrates the vertical gust profile for varying gust frequencies (F) and magnitudes (WG).

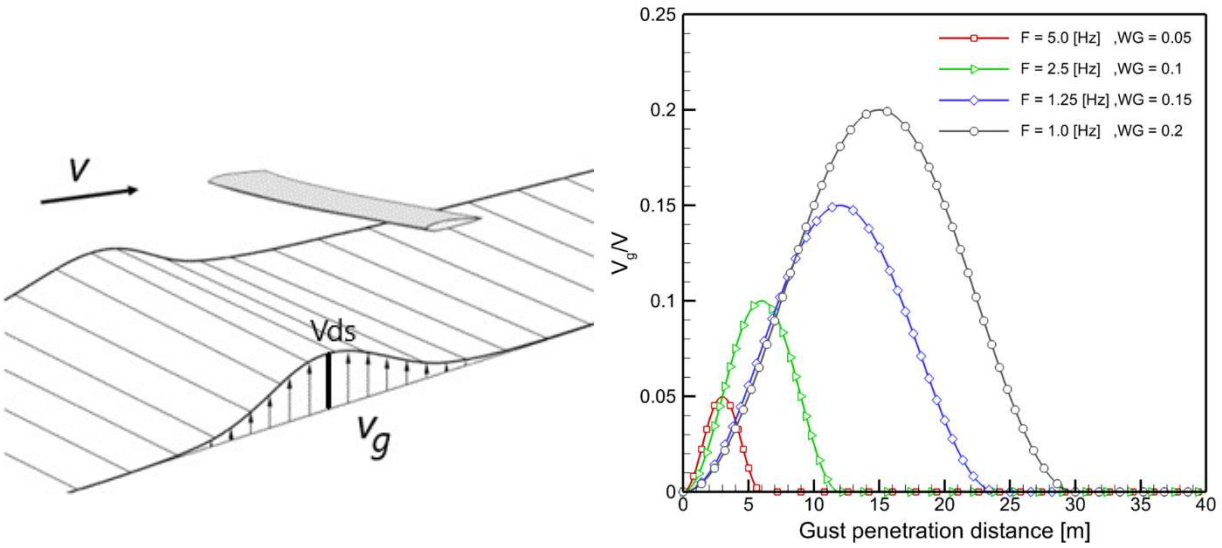

Figure 4. Vertical gust profile for different gust frequencies and magnitudes

The induced downwash $w_g(t)$ due to the gust is given by $dV_g(t)/dt$. This equation captures how the gust's intensity changes with time, influencing the wing's aerodynamic environment.

Consequently, the aerodynamic force due to the gust can be represented as $\mathbf{F}_{gust}(t) = \mathbf{Q}(k)\mathbf{W}(t)$, where $\mathbf{W}(t)$ is the gust-induced downwash distribution over the wing. The coupled equations of motion for the aeroelastic system in modal coordinates are described by;

$$\mathbf{M}\ddot{\mathbf{q}}(t) + \mathbf{C}\dot{\mathbf{q}}(t) + \mathbf{K}\mathbf{q}(t) = \mathbf{F}_{aero}\big(\mathbf{q}(t), \dot{\mathbf{q}}(t)\big) + \mathbf{F}_{gust}(t) \tag{2}$$

where $\mathbf{q}(t)$ is the vector of modal coordinates, $\mathbf{C}$ the damping matrix, and $\mathbf{F}_{aero}$ includes the aerodynamic forces due to structural deformation and velocity. The aerodynamic forces are further defined as $\mathbf{F}_{aero} = \mathbf{A}(t)\mathbf{q}(t) + \mathbf{B}(t)\dot{\mathbf{q}}(t)$, where $\mathbf{A}(t)$ and $\mathbf{B}(t)$ are matrices representing the influence of structural deformation and velocity on aerodynamic forces.

A ROM is constructed using the mode shapes ϕ_n and natural frequencies ω_n obtained from ANSYS. The dynamic response is represented in terms of the modal coordinates as $\mathbf{u}(t) = \sum_{\boldsymbol{n}} \phi_n \mathbf{q}_n(t)$.

For solving the gust response, ZAERO is employed to simulate the time-domain response of the ROM to the gust input. The coupled equations of motion are integrated numerically to obtain the time history of the modal coordinates $\mathbf{q}_n(t)$. Post-processing involves transforming the modal response back to physical coordinates to analyze displacements, velocities, and stresses in the wing structure. This step is crucial for assessing the impact of the gust on the wing's performance and structural integrity.

4.2 Modeling the wingtips in ANSYS

The process of modeling the wing in ANSYS begins with the creation of a detailed CAD model of the main wing and wingtip, ensuring that pivot points and hinges are accurately defined. This model is subsequently imported into ANSYS DesignModeler, where appropriate material properties are assigned to the components. In ANSYS Workbench, a revolute joint with specified torsional stiffness is defined under the "connections" module between the main wing and the wingtip. The rotational degree of freedom and the torsional stiffness of the joint are carefully specified. During the translation to APDL, it is crucial to ensure that this joint is represented by an MPC184 element. The MPC184 element effectively models the revolute joint with the defined torsional stiffness, accurately simulating the spring mechanism's behavior in the folding process. This configuration allows the wingtip to fold/twist under aerodynamic gust loads while providing resistance through the torsional spring.

The geometry is then meshed, with particular attention to creating finer elements around the joint and spring attachment areas to capture detailed behaviors. A modal analysis is performed to extract eigenvalues and eigenvectors, which are essential for subsequent gust analysis using ZAERO based on the ROM method.

5 RESULTS AND DISCUSSION

The following sections undertake a comprehensive examination of the influence of wingtip devices on the alleviation of gust loads. Specifically, these sections analyze the influence of FWT and TWT on Root Bending Moment (RBM), respectively.

5.1 The effect of FWT on GLA

Figures 5a and 5b illustrate the time response of the fold angle (β) for a FWT with two different flare angles: 10° and 20°. These configurations are subjected to a 1-cosine gust model with an amplitude of 0.1 and a gust length of 25c, while maintaining a wingtip length of 250 mm and for k_β=5, 10, 20, 100 Nm/rad. An initial observation reveals that a lower flare angle corresponds to a slightly greater range of motion variation.

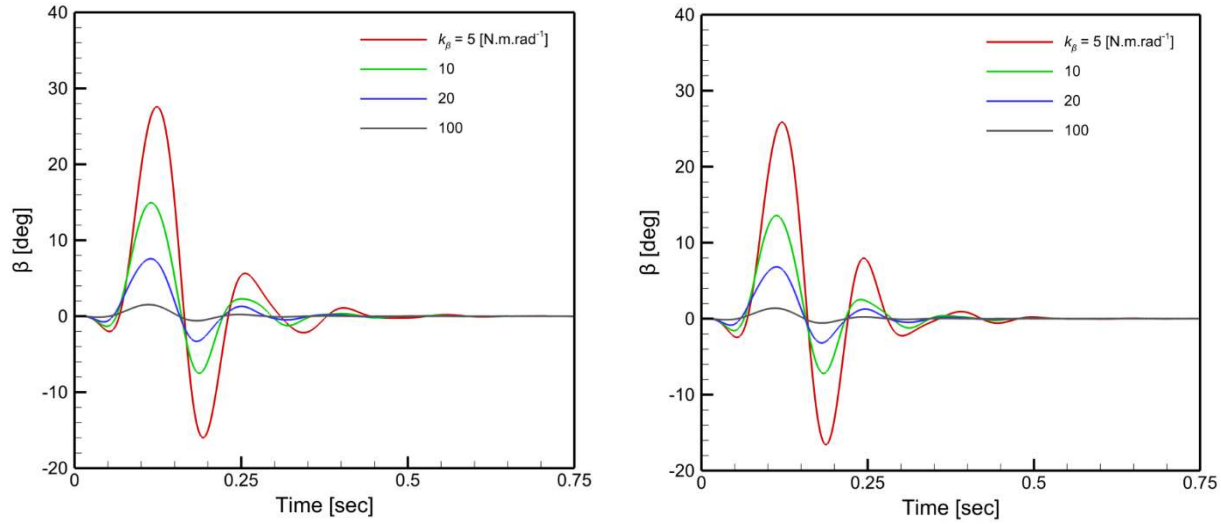

(a) (b)

Figure 5. Fold angle (β) response for FWT subjected to 1-cosine gust with $WG = 0.1$, $2H =$ 25c, wingtip length $L_F = 250$ mm and a) $\Lambda = 10^{\circ}$ and b) $\Lambda = 20^{\circ}$

Figure 6a and 6b provide a comparison of the results for the RBM for Folding wing with flare angle of 10° and 20°, while keeping the wingtip length constant at 250 mm. The calculations incorporate different spring stiffness values k_β=5, 10, 20, 100 Nm/rad. In general, the findings indicate a reduction in the maximum peak RBM when employing a FWT in comparison to the baseline configuration. As the stiffness value increases from 5 to 100 Nm/rad, the favorable impact of the wingtip on GLA diminishes.

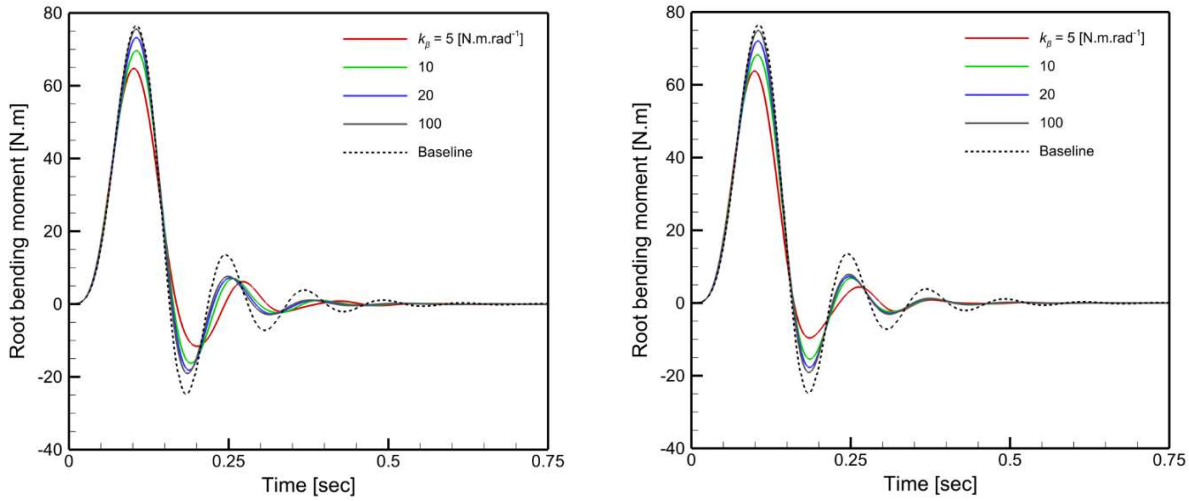

(a) (b)

Figure 6. RBM (M_x) time response for FWT subjected to 1-cosine gust with $WG = 0.1$, $2H =$ 25c, wingtip length of $L_F = 250$ mm and a) $\Lambda = 10^{\circ}$ and b) $\Lambda = 20^{\circ}$

Figure 7 examines the effect of the length of wingtip (L_F). The length of the wingtip makes a significant difference in reducing maximum pick in bending moment. However, what matters just as much is what percentage the length of the wingtips is compared to the whole wing. When the wingtips are more than 10% of the wing length, they work really well at reducing the loads.

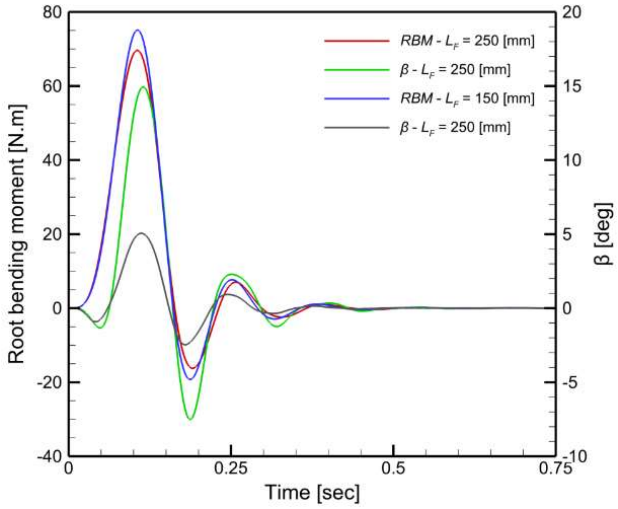

Figure 7. RBM (M_x) and Fold angle (β) response for FWT subjected to 1-cosine gust with $WG = 0.1$, $2H = 25$c, k_β=10 N.m.rad^{-1}, Λ=10° and wingtip length of $L_F =$ 150 mm and 250 mm

5.2 The effect of TWT on GLA

This section explores how a TWT device affects the performance of GLA. The starting point for comparison is the baseline wing configuration which serves as the reference model for this analysis.

The time response of a Twist wing is assessed, considering two distinct hinge positions in Figure 8a and 8b; 10 mm and 30 mm, respectively. This is done while maintaining a wingtip length of 250 mm and considering spring stiffness values of k_θ=5, 10, 20, 100 Nm/rad. In this context, a positive twist angle corresponds to an upward rotation of the wingtip, while a negative twist angle corresponds to a downward rotation resulting in a decrease in the angle of attack. Notably, the smallest spring stiffness yields the maximum twist angle observed.

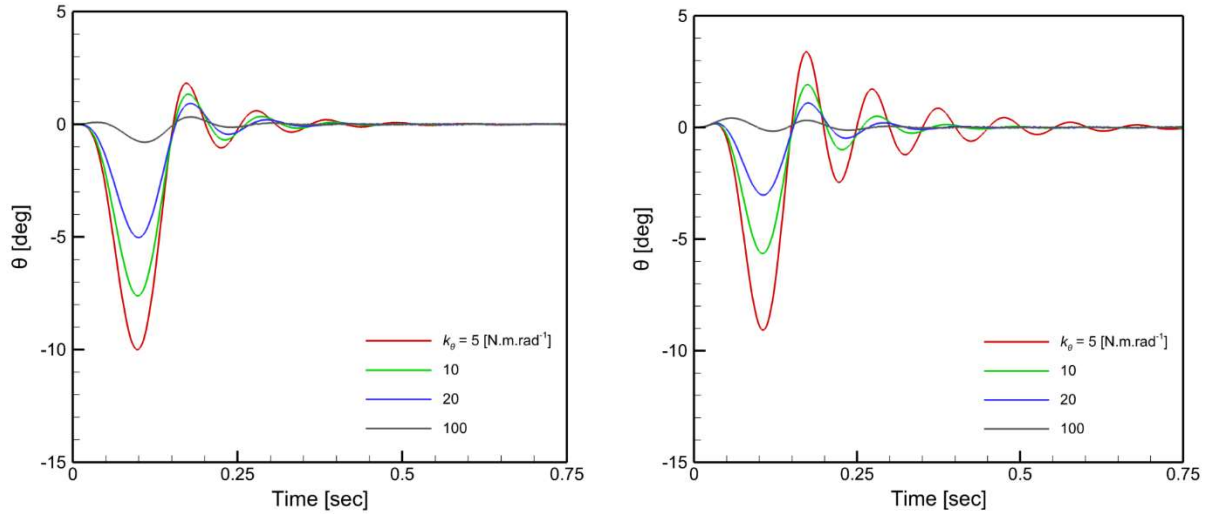

(a) (b)

Figure 8. Twist angle (θ) time responses for TWT subjected to 1-cosine gust with $WG = 0.1$, $2H = 25$c, $L_T = 250$ mm and hinge position of, a) $h = 10$ mm, b) $h = 30$ mm

Figure 9 illustrates the RBM response of a Twist wing subjected to gust loading, considering two hinge position; 10 mm and 30 mm. A decrease in spring stiffness leads to a greater reduction in the maximum peak RBM. Notably, a significant enhancement in GLA is observed between the baseline configuration and the Twist wing with a spring stiffness of 5 Nm/rad. This improvement results in a reduction of the RBM by 123% and 61% for hinge position of 10 mm and 30 mm, respectively.

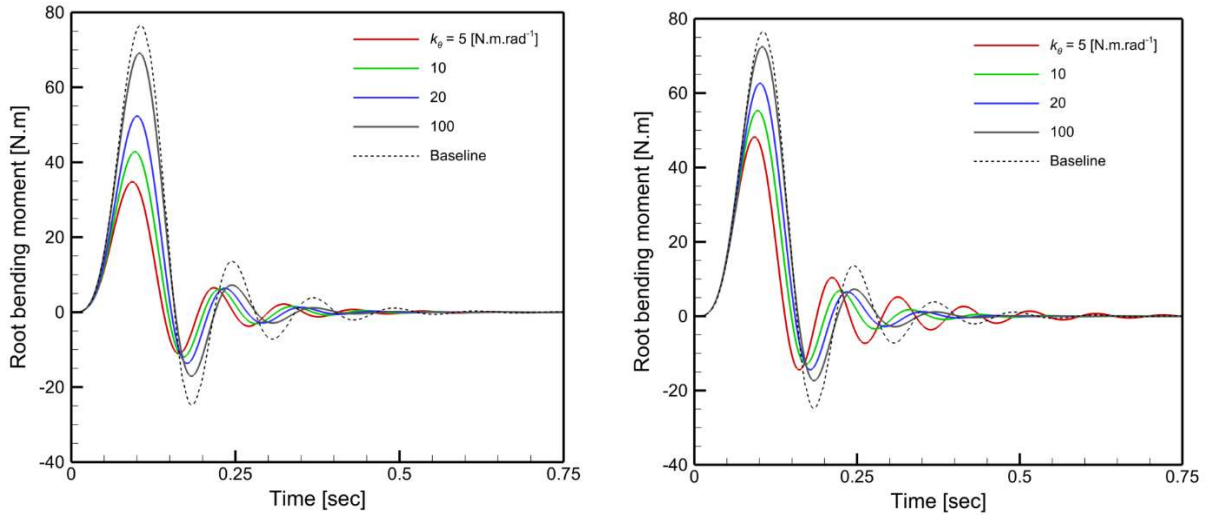

(a) (b)

Figure 9. RBM (M_x) time response for TWT subjected to 1-cosine gust with $WG = 0.1$, $2H = 25$c, wingtip length of $L_T = 250$ mm and a) h =10 mm and b) h =30 mm

Figure 10 explores the impact of wingtip length (L_T) in hinge positions, h=10 mm on GLA. The length of the wingtips plays a crucial role in altering the maximum peak in RBM.

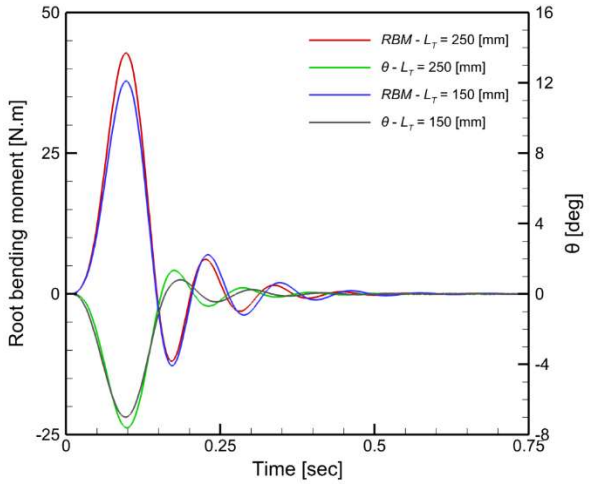

Figure 10. RBM (M_x) and Twist angle (θ) response for TWT subjected to 1-cosine gust with $WG = 0.1$, $2H = 25$c, k_θ=10 N.m.rad^{-1}, h=10 mm and wingtip length of $L_T =$ 150 mm and 250 mm

In conducting a parametric investigation, the impact of hinge position (h), spring stiffness (k_θ), and wingtip length (L_T) on the RBM within the context of a TWT configuration is explored in Figures 11a. Similarly, the RBM within the context of a FWT configuration, as depicted in Figure 11b, is investigated with respect to flare angle (Λ), spring stiffness (k_β), and wingtip length (L_F).

In Figure 11a and 11b, it is observed that, within a range of spring stiffness values for all twist and flare angles, the wingtips demonstrate optimal performance in reducing gust-induced loads and minimizing RBM compared to the baseline wing. As the spring stiffness exceeds a certain threshold, the bending moment almost converges to results obtained from the baseline wing. Lower values of spring stiffness correspond to reduced bending moments. For TWT, Generally, enhancing GLA performance involves reducing spring stiffness and positioning the hinge closer to the leading edge. For FWT, the increase in wingtip length enhances the efficiency of the wingtip in reducing bending moments compared to the baseline wing. Additionally, an increase in flare angle more contributes to the reduction of the RBM.

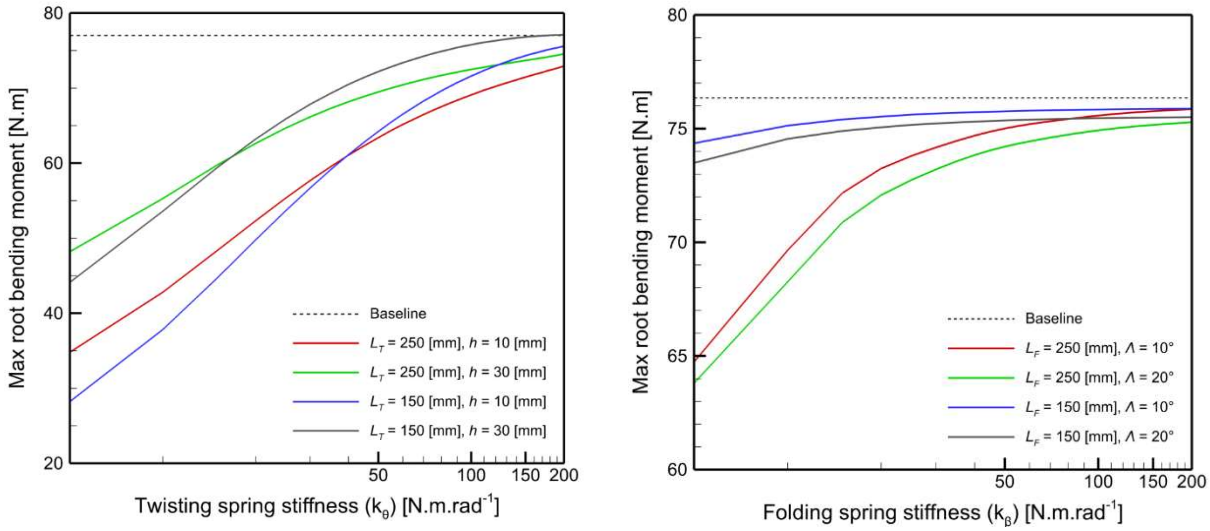

(a) (b)

Figure 11. RBM (M_x) versus a) spring stiffness (k_θ) for TWT and b) spring stiffness (k_β) for FWT subjected to 1-cosine gust with $WG = 0.1$, $2H = 25$c

5 CONCLUSIONS

Wingtip devices, such as Twist and Folding wing configurations, have become a research topic in aerospace engineering research, especially since high aspect ratio wing designs have been recognized and validated as effective for reducing weight and improving aircraft endurance. The integration of three distinct analysis tools within the NAS^2 package enables comprehensive simulations. Subsequently, TWT and FWT devices are incorporated into the baseline wing model developed in Ref. [7], demonstrating the effectiveness of these wingtip devices in enhancing GLA performance. When comparing TWTs and FWTs, it becomes clear that TWTs are more effective at reducing RBM, especially when the hinge is positioned near the leading edge. However, this design increases complexity because it requires careful adjustment of the spring stiffness and selection of the wingtip length. On the other hand, FWTs are simpler to design than TWTs. Generally, FWTs achieve a lower RBM comparing to baseline wing.

ACKNOWLEDGMENT

This study has been supported by the Scientific and Technological Research Council of Türkiye (TÜBİTAK, Project No. 220N396 and TÜBİTAK 2219 program). The authors gratefully acknowledge the support of this study.

REFERENCES

[1] Farsadi, T., Rahmanian, M., & Kayran, A. (2018). Geometrically nonlinear aeroelastic behavior of pretwisted composite wings modeled as thin walled beams. *Journal of Fluids and Structures, 83,* 259-292.

[2] Farsadi, T., Rahmanian, M., & Kayran, A. (2020). Reduced order nonlinear aeroelasticity of swept composite wings using compressible indicial unsteady aerodynamics. *Journal of Fluids and Structures, 92,* 102812.

[3] Sina, S. A., Farsadi, T., & Haddadpour, H. (2013). Aeroelastic stability and response of composite swept wings in subsonic flow using indicial aerodynamics. *Journal of Vibration and Acoustics, 135(5),* 051019. 57.

[4] Asadi, D., Farsadi, T., & Kayran, A. (2021). Flutter optimization of a wing–engine system with passive and active control approaches. *AIAA Journal, 59(4),* 1422-1440.

[5] Asadi, D., & Farsadi, T. (2020). Active flutter control of thin walled wing-engine system using piezoelectric actuators. *Aerospace Science and Technology, 102,* 105853.

[6] Ahmadi, M., & Farsadi, T. (2024). Multidisciplinary optimization of high aspect ratio composite wings with geometrical nonlinearity and aeroelastic tailoring. *Aerospace Science and Technology, 145,* 108849.

[7] Farsadi, T., Ahmadi, M., Sahin, M., Haddad Khodaparast, H., Kayran, A., & Friswell, M. I. (2024). High Aspect Ratio Composite Wings: Geometrically Nonlinear Aeroelasticity, Multi-Disciplinary Design Optimization, Manufacturing, and Experimental Testing. *Aerospace, 11(3),* 193.

[8] Castrichini, A., Siddaramaiah, V. H., Calderon, D. E., Cooper, J. E., Wilson, T., & Lemmens, Y. (2017). Preliminary investigation of use of flexible folding wing tips for static and dynamic load alleviation. *The Aeronautical Journal, 121(1235),* 73-94.

[9] Gu, H., Healy, F., Rezgui, D., & Cooper, J. (2023). Sizing of High-Aspect-Ratio Wings with Folding Wingtips. *Journal of Aircraft, 60(2),* 461-475.

[10] Healy, F., Cheung, R., Rezgui, D., Cooper, J., Wilson, T., & Castrichini, A. (2023). Experimental and Numerical Nonlinear Stability Analysis of Wings Incorporating Flared Folding Wingtips. *Journal of Aircraft,* 1-15.

[11] Carrillo Córcoles, X., Mertens, C., Sciacchitano, A., van Oudheusden, B. W., De Breuker, R., & Sodja, J. (2023). Effect of Wing Stiffness and Folding Wingtip Release Threshold on Gust Loads. *Journal of Aircraft,* 1-20.

[12] Cheung, R. C., Rezgui, D., Cooper, J. E., & Wilson, T. (2018). Testing of a hinged wingtip device for gust loads alleviation. *Journal of Aircraft, 55(5),* 2050-2067.

[13] Balatti, D., Haddad Khodaparast, H., Friswell, M. I., Manolesos, M., & Amoozgar, M. (2022). The effect of folding wingtips on the worst-case gust loads of a simplified aircraft model. *Proceedings of the Institution of Mechanical Engineers, Part G: Journal of Aerospace Engineering, 236(2),* 219-237.

[14] Balatti, D., Khodaparast, H. H., Friswell, M. I., Manolesos, M., & Castrichini, A. (2023). Experimental and numerical investigation of an aircraft wing with hinged wingtip for gust load alleviation. *Journal of Fluids and Structures, 119,* 103892.

[15] Ajaj, R. M., Saavedra Flores, E. I., Amoozgar, M., & Cooper, J. E. (2021). A parametric study on the aeroelasticity of flared hinge folding wingtips. *Aerospace, 8(8),* 221.

[16] He, S., Guo, S., Liu, Y., & Luo, W. (2021). Passive gust alleviation of a flying-wing aircraft by analysis and wind-tunnel test of a scaled model in dynamic similarity. *Aerospace Science and Technology, 113,* 106689.

[17] Guo, S., Jing, Z. W., Li, H., Lei, W. T., & He, Y. Y. (2017). Gust response and body freedom flutter of a flying-wing aircraft with a passive gust alleviation device. *Aerospace Science and Technology, 70,* 277-285.

[18] Ahmadi, M., Farsadi, T., & Khodaparast, H. H. (2024). Enhancing Gust Load Alleviation Performance in an Optimized Composite Wing using Passive Wingtip Devices: Folding and Twist Approaches. *Aerospace Science and Technology,* 109023.

COPYRIGHT STATEMENT